2016-01-0672

Fuel Economy Gains through Dynamic-Skip-Fire in Spark Ignition Engines

Kian Eisazadeh-Far, Matthew Younkins
Tula Technology Inc.

Abstract

Pumping losses are one of the primary energy losses in throttled spark ignition engines. In order to reduce fuel consumption, engine manufacturers are incorporating devices that deactivate the valve-train in some cylinders. In the operating strategies currently implemented in the market, fixed sets of cylinders are deactivated, allowing 2 or 3 operating modes. In contrast, Tula Technology has developed Dynamic Skip Fire (DSF), in which the decision of whether or not to fire a cylinder is decided on a cycle-by-cycle basis. Testing the DSF technology in an independent certified lab on a 2010 GMC Denali, reduces the fuel consumption by 18% on a cycle-average basis, and simultaneously increases the ability to mitigate noise and vibration at objectionable frequencies.

This paper outlines the results of the experiments that have been conducted on an eight cylinder engine over a wide range of conditions to investigate the fuel consumption gains and emissions impact when incorporating DSF technology. The experiments have been carried out over a wide range of engine speeds, loads, and DSF strategies and significant improvements have been observed.

Introduction

Pumping losses are one of the major sources of thermal efficiency losses in spark ignition engines. Cylinder deactivation reduces the pumping losses by deactivating cylinders during every engine cycle based on torque requirements.

As a means to improve engine efficiency, cylinder deactivation has a long history. It has been employed by General Motors's Active Fuel Management (AFM) system in eight cylinder engines [1]. In their approach, four of eight cylinders are deactivated in a 5.3L or 6.2L OHV V8 engine; meaning that a fixed pattern of deactivation is applied and fully implemented in each engine cycle. Other OEMs have also used cylinder deactivation [2-3]. For instance in VW's 1.4-liter TSI 4-cylinder engine, cylinders 2 and 3 are deactivated [2]. Similar to [1], in VW's engine a fixed pattern of deactivation is implemented and completed in each engine cycle. In this firing pattern, a deactivated cylinder is always followed by a firing cylinder event in each engine cycle. Although firing every other cylinder is the most common approach, some deactivation strategies have used other approaches. For instance, Honda has fired two out of every three cylinders in a 3.5L i-VTEC engine [3].

At Tula Technology, we have introduced Dynamic Skip Fire (DSF) an evolved version of deactivation which is capable of deactivating the cylinders without any limitation. DSF deactivates cylinders in a manner that achieves the load demanded while avoiding objectionable noise and vibration. For example, Figure 1 displays a DSF pattern of 1 fire followed by 2 skips for each cylinder. Figure 1 shows that three cycles are required to achieve this pattern.

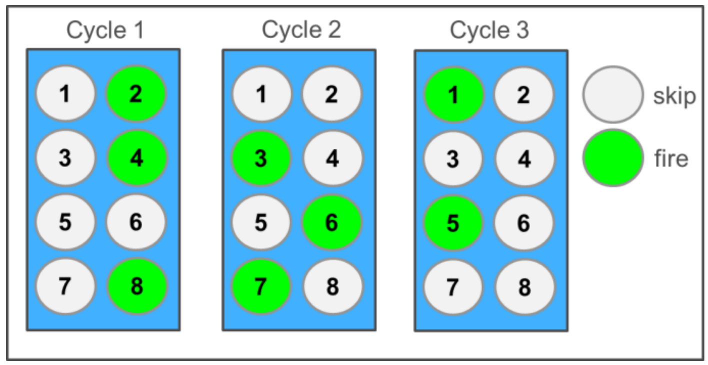

Figure 1: DSF operation of 1 fire - 2 skips for each cylinder in an eight cylinder engine

Along with rewarding achievements of DSF, there are also some challenges. Choosing the firing density based only upon fuel economy would induce undesirable NVH characteristics. Each fire induces a torque which creates an acceleration exerted to the crankshaft. The acceleration causes vibrations whose frequency is a function of firing density and firing pattern. Due to the variable nature of DSF in terms of firing frequency, great care should be taken to avoid frequencies in which perception of vibration or resonance is encountered. More details about evaluation and mitigation of NVH in Tula DSF can be found in [5].

One of the benefits of DSF is the wide range of firing pattern selections to minimize the resonance modes. This capability of DSF provides us the opportunity to choose firing patterns which produce surprisingly lower NVH than V8 at equivalent power. Besides NVH considerations, our FTP cycle data for L94 engine (employed in 2010 GMC Denali) show fuel economies of 19.92 mpg at DSF versus 17.34 mpg at V8 mode. Meaning, DSF reduces fuel consumption by 14-18% over V8 [6].

In Tula's previous publications (e.g. [5, 6]), the fundamental concepts of DSF, have been discussed. In this paper we are presenting a comparative study of DSF advantages versus V8 mode. We will discuss the results in a wide range of operational conditions (listed in

Table 2). The main focus of this paper will be on fuel economy, DSF impacts on combustion stability, and pollutant emissions.

Experimental Setup

For the experiments in this paper, Tula Technology used a production General Motors L94 6.2L V8 engine, modified by Tula to be compatible with Dynamic Skip Fire. The base engine was used by General Motors in many applications, among them, the 2010 GMC Yukon Denali. The hardware modifications required for DSF were:

1. Addition of production lost-motion lifters for cylinder deactivation, required for both intake and exhaust valves for the four cylinders not equipped with these lifters from General Motors
2. Modification to the engine block to allow oil routing to each of the lost-motion lifters
3. Fabrication of a new lifter oil manifold assembly, including a solenoid system to direct oil to the control port of the added lost-motion lifters.

Table 1 lists the specifications of Tula's DSF Engine.

Table 1. Specifications of Tula Technology Dynamic Skip Fire Engine

Type	V8
Displacement	6162 cm3
Bore and stroke	103.25 mm x 92 mm
Block material	cast aluminum
Cylinder head material	cast aluminum
Valvetrain	overhead valve, two valves per cylinder, dual-equal variable cam phasing
Deactivation system	Intake and exhaust lost-motion lifters, oil pressure actuated
Ignition system	coil-near-plug ignition
Fuel delivery	Port injected, sequential
Compression ratio	10.4:1
Power (peak)	301 kW @ 5700 rpm
Torque (peak)	565 N.m @ 4300 rpm
Maximum speed	6000 rpm

Dynamic Skip Fire

Tula's DSF minimizes the pumping losses by deactivating a number of cylinders while acceptable NVH limits are maintained. Throughout this process, the air mass is increased in each firing cylinder to produce more torque. By doing so, the manifold pressure is elevated to lower the pumping losses. The net amount of DSF engine torque in elevated manifold pressure equals the net V8 engine torque in throttled condition. Pumping loss is defined as:

$$W_P = (p_i - p_e)(V_i - V_e) \tag{1}$$

where p_i and p_e are intake and exhaust pressures, V_i and V_e are TDC and BDC volumes of engine. When p_i approaches to p_e, W_p will decrease. In Figure 2, a comparison of DSF and V8 operation at a common load is shown (BMEP = 1.8 bar @ 1600 rpm). DSF operation is for the event shown in Figure 1 (1 fire followed by two skips). At the same BMEP the amount of pumping losses incurred by DSF are significantly lower than V8 operation.

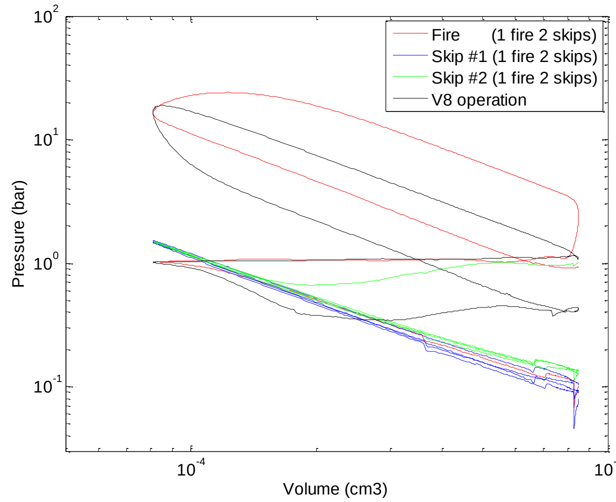

Figure 2: p-v diagram of DSF (firing pattern shown in figure 1) and V8 operation, BMEP = 1.8 bar @ 1600 rpm

Figure 3 shows the contour plots of manifold pressure versus BMEP and engine speed for DSF and V8 operations. Figure 3 involves several firing densities ranging from 10% to 100% (firing density is the ratio of firing events at DSF to V8 mode; for example firing density of DSF mode in Figure 2 is 1/3). Table 2 shows the experimental matrix of the tests used for Figures 3. Since DSF operation substantially increases manifold pressure, pumping losses are minimized. Contour plots of Figure 4 show the PMEP of DSF and V8 operations; significant reductions in DSF pumping losses are seen in this figure.

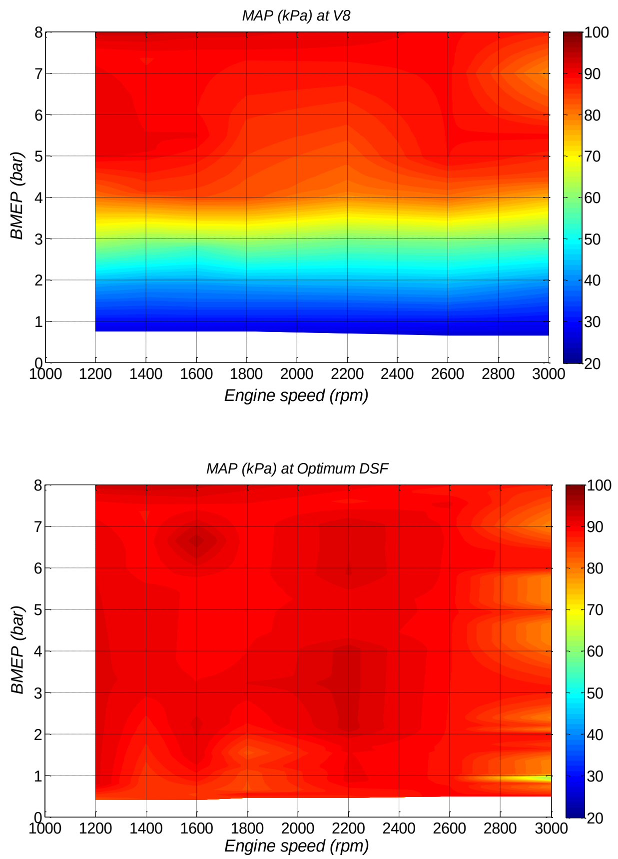

Figure 3: The contour plots of manifold pressure for V8 and DSF operations as a function of BMEP and engine rpm (test matrix shown in Table 2)

Table 2: Test matrix of the contour plots

Engine speed	1200:200:3000 rpm
Manifold pressure	25:10:100 kPa
Firing density	1/9:1
CAM phasing (optimized for the best BSFC)	0:50 degrees
Spark Timing (optimized for the best BSFC based on knock limits)	9:55 CAD

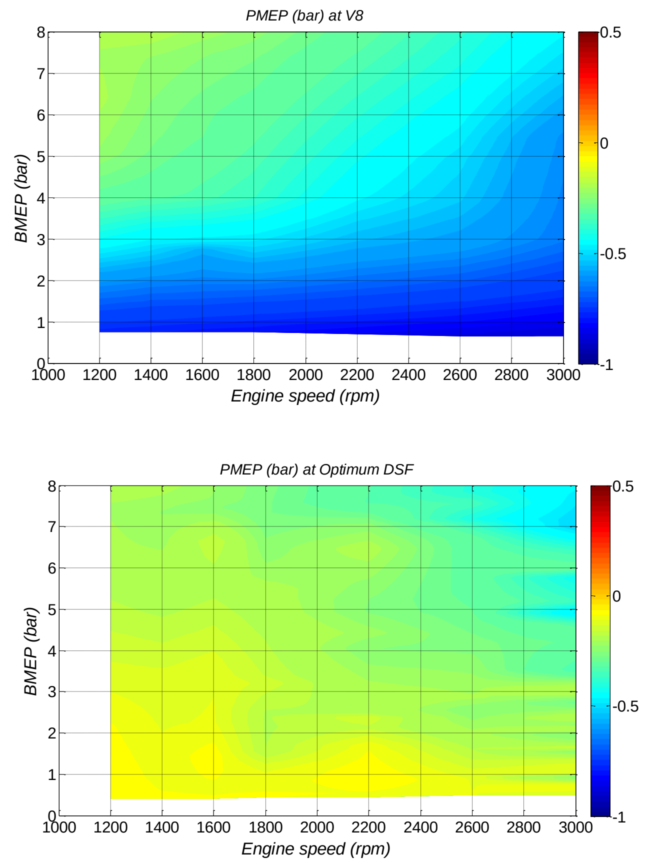

Figure 4: The contour plots of pumping loss for V8 and DSF operations as a function of BMEP and engine rpm (test matrix shown in Table 2)

Fuel Economy gains through DSF

Shown in Table 2, we have tested a wide range of conditions including dozens of firing densities, engine speeds, and manifold pressures. All tests were conducted at optimum camshaft position and spark timing for the best BSFC considering the knock limits.

Figure 5 shows the experimentally determined BSFC of the engine as a function of BMEP at 1400 rpm. Many firing densities were tested; these points are shown in blue edge color symbols marked as "all firing densities". Figure 5 shows that, for a given engine load, several firing densities are possible. However, only one of those firing densities has the optimum BSFC. Those optimal points are marked in red as "Optimum DSF". Figure 6 explicitly shows the advantage in fuel consumption that Tula DSF has when compared to base V8 engine operation. It can be seen that at low BMEPs we experience the highest fuel savings by running DSF.

Figures 7 and 8 show the contour plots of BSFC and fuel flow for all engine speeds at all conditions. All points are for V8 and optimum DSF. Figure 8 presents the significant fuel economy gains of DSF at low loads. Figure 8 shows that there is up to 60% gains in fuel flow (g/s) operating DSF. It should be noted that Figures 5-8 do not involve NVH considerations. Optimum firing densities are modified based on NVH features to be used in the vehicle.

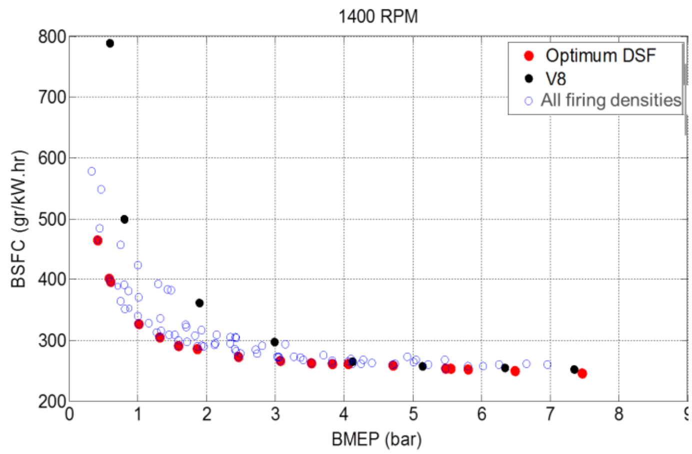

Figure 5: BSFC (gr/kW.hr) of engine in various DSF modes as a function of BMEP at 1400 rpm

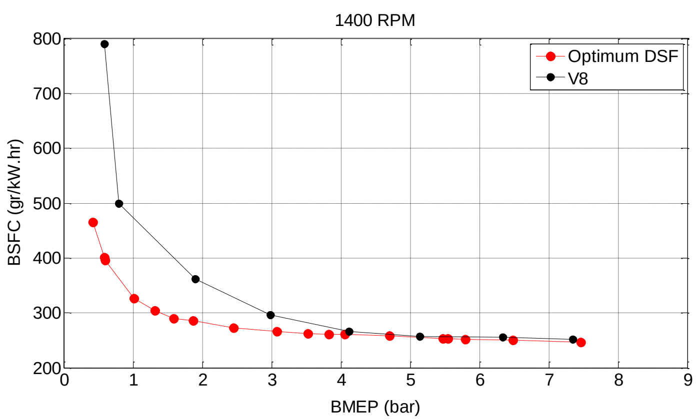

Figure 6: BSFC (gr/kW.hr) of engine in optimum DSF mode as a function of BMEP at 1400 rpm

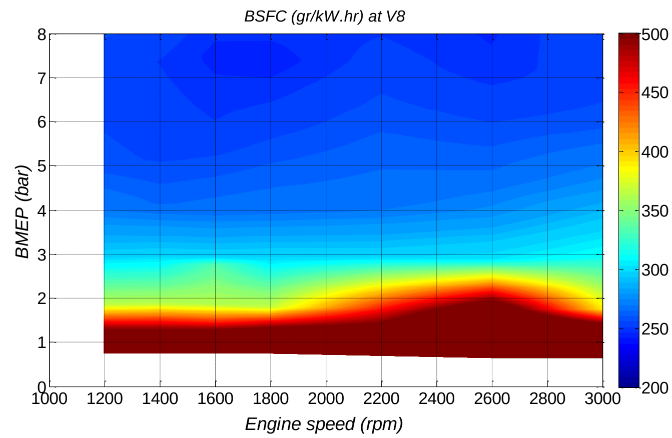

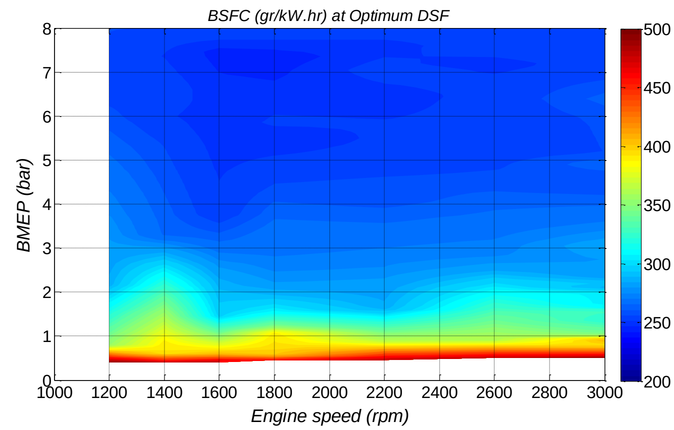

Figure 7: BSFC (gr/kW.hr) contour plots of V8 and DSF operations

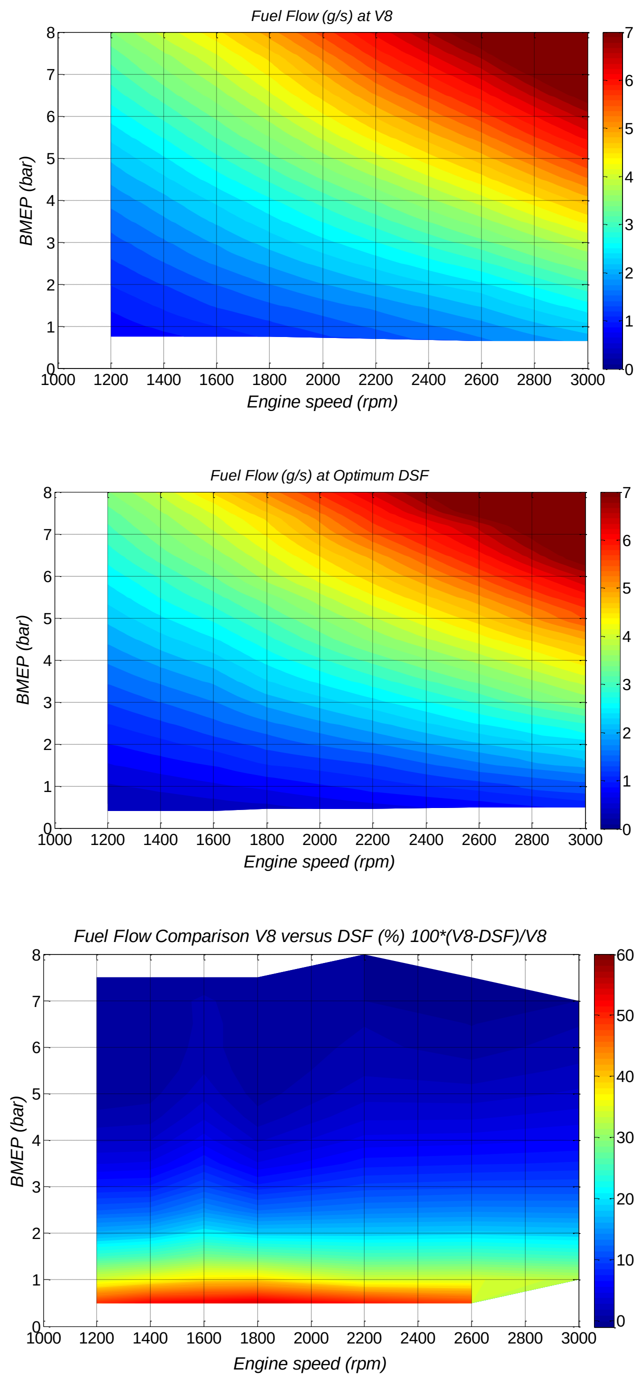

Figure 8: contours of fuel flow (g/s) of V8 and optimum DSF operations as a function of BMEP and rpm

DSF and combustion stability

DSF does not fundamentally change the thermodynamic cycle of an engine. Nevertheless, due to the new paradigm of an engine where a cylinder is fired or not on an as-needed basis, DSF may have some impacts on the combustion stability of each cylinder. Figure 9 compares the runner pressure of a particular cylinder that has fired once after skipping twice. The V8 intake runner pressure is shown for comparison. Although both experiments were run with a cycle-average manifold pressure of 90 kPa, the instantaneous pressure within the runner for DSF and V8 are distinct. The difference in the pattern of runner pressure (and generally manifold pressure) for DSF and V8 can be explained by different pressure pulses from cylinders due to activation and deactivation processes. It should be noted that manifold dynamics has a significant impact on volumetric efficiency of each cylinder [7]. The impact of cylinder deactivation on volumetric efficiency was studied by Ohata and Ishida [8]; it was shown that the profile of manifold pressure 30 degrees before inlet valve closing (IVC) time can affect the volumetric efficiency tremendously. Different volumetric efficiencies of DSF versus V8 will cause variations in combustion process in each cylinder. Figure 10 shows the variations of net mean effective pressure (NMEP) of engine as a function of firing density. Figure 10 indicates that NMEP of each firing cylinder will vary as a function of firing density. The variations with respect to V8 mode is about +-4%. We have conducted a thorough test of the engine at many firing densities to incorporate these effects in engine control structure [9]. It has produced a smooth performance of DSF at relevant conditions while maintaining production NVH quality [5].

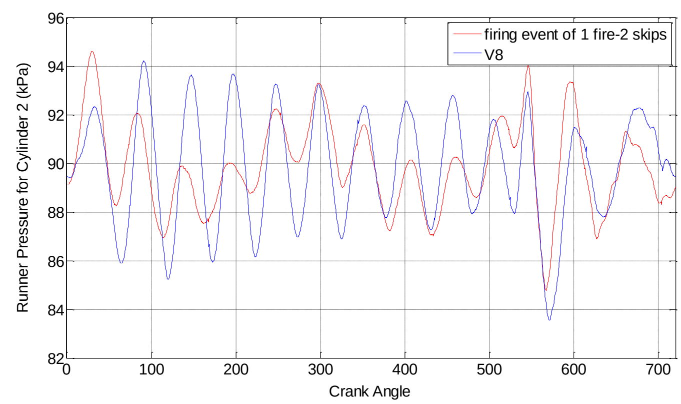

Figure 9: Runner pressure comparison of cylinder 2 for DSF pattern of 1 fire-2 skips versus V8 @ 1500 rpm, manifold pressure = 90 kPa

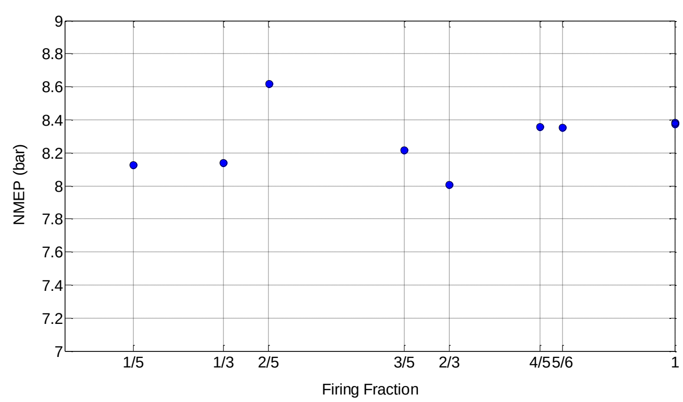

Figure 10: Average NMEP as a function of firing fraction at 1500 rpm, Manifold Pressure = 90 kPa

In addition to manifold dynamics, other factors can also contribute in cycle-to-cycle variations. The variations of gas dynamics within cylinder during combustion, variations of fuel composition and mixture stoichiometry in each cycle, and the quality of flame formation and propagation in the vicinity of spark plug can cause cycle-to-cycle variations [10]. Also, running V8 will cause an overlap in intake and exhaust valve depending on cam phasing whereas at some firing densities DSF will not experience overlapping due to deactivation of the cylinder. In order to evaluate the repeatability and stability of combustion in firing events, coefficient of variation for indicated mean effective pressure (IMEPCOV) is calculated for each case over a number of cycles. IMEPCOV is defined as:

$$\mathbf{IMEPCOV} = \frac{\mathbf{100}}{\boldsymbol{IMEP_{(avg)}}} \sqrt{\frac{\boldsymbol{n} \sum_{j=n}^{i} (\boldsymbol{IMEP_j})^2 - \left(\sum_{j=n}^{i} \boldsymbol{IMEP_j}\right)^2}{\boldsymbol{n}(\boldsymbol{n}-\mathbf{1})}} \qquad (2)$$

where n is the number of cycles, and $IMEP_{(avg)}$ is the mean IMEP over n cycles. In our tests n = 300. Usually for eight cylinder engines IMEPCOVs below 0.05 represents acceptably stable combustion over n cycles.

Figure 11 compares the IMEPCOVs during DSF and conventional operation. For both cases, the engine calibration is such that acceptable IMEPCOV is obtained. For conventional operation, IMEPCOV is high at low BMEPs; high residual fraction and minimal fresh charge increases the likelihood of misfiring. In contrast, DSF improves IMEPCOV at low BMEP by improving combustion and reducing the chance of misfire. In some regions, DSF is experiencing relatively higher IMEPCOVs (e.g. 2200-2600 rpm, BMEP: 4-5 bars). As it was discussed in Figure 9, it can be due to different volumetric efficiencies of each firing cylinder. A good calibration of engine at DSF can maintain IMEPCOVs in an acceptable limit. Shown in Figure 12, IMEP of each firing event in V8 mode and DSF mode are compared over 300 cycles. It is observed that for the same BMEP, V8 causes higher variations in IMEP than DSF. It will have significant fuel economy penalties at V8. One of the major reasons for IMEP variations is poor combustion or misfiring. Misfiring phenomenon is not the main scope of this paper. Tula engineers have thoroughly investigated misfiring in Dynamic Skip Fire and have several algorithms that have been shown to be robust to that phenomenon [11].

Operating DSF can impact combustion rate in the cylinder. DSF increases the pressure of the charge inside the cylinder, consequently the combustion pressure. Pressure changes the rate of burning [10]. The benefit of DSF at low loads is that it increases the mass of air in the cylinder which will enhance stable combustion. Stable combustion improves the burning process causing faster release of fuel energy. Figure 13 shows the combustion duration 10% to 90% (deg) for V8 and DSF operation. As it can be seen at intermediate to high loads (bmep > 4 bar), combustion durations of V8 and DSF are close. At low loads, combustion duration is longer for V8. It can be attributed to more stable combustion at DSF. It is well known that higher heat release rate enhances the thermal efficiency in spark ignition engines [10].

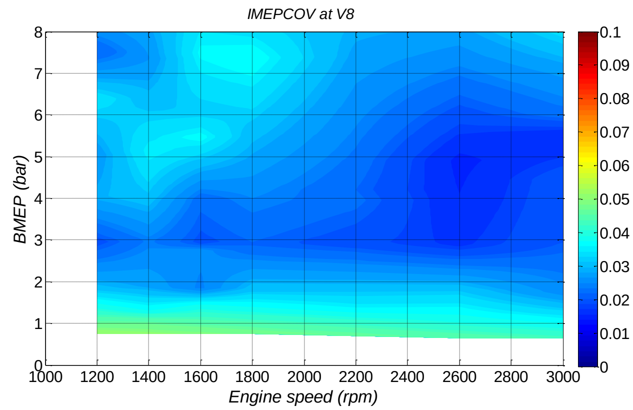

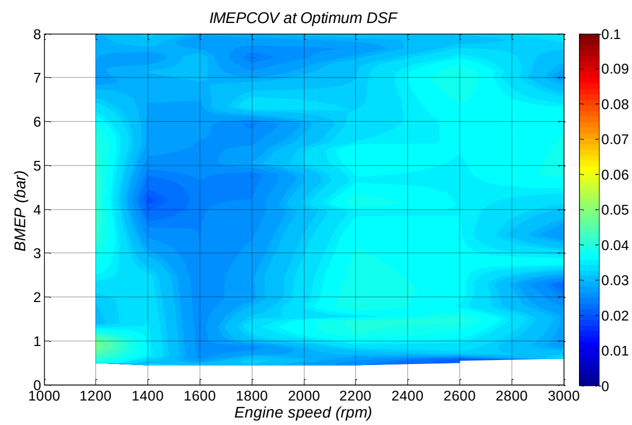

Figure 11: Contour plot of IMEPCOV of V8 and DSF modes as a function of BMEP and rpm (test matrix shown in Table 2)

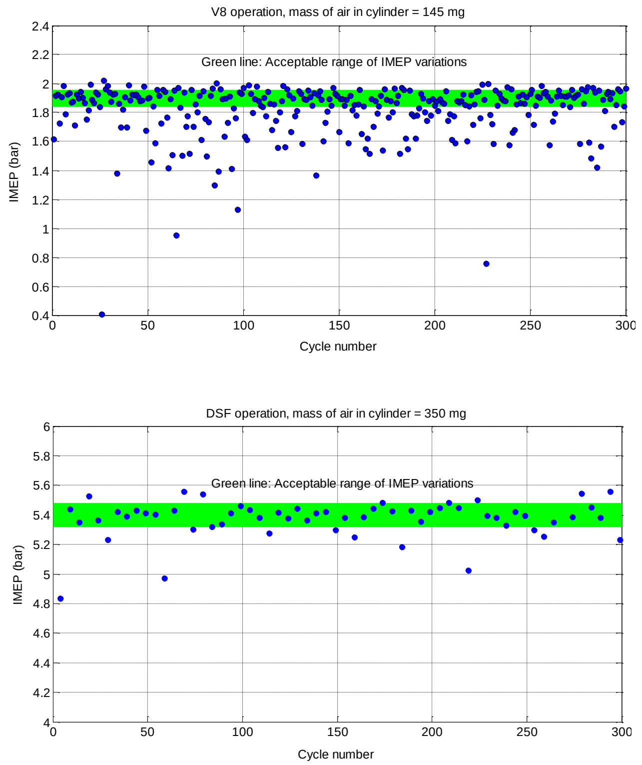

Figure 12: IMEP variations over 300 cycles, 1400 rpm, BMEP = 0.65 bar, operating at V8 and DSF modes

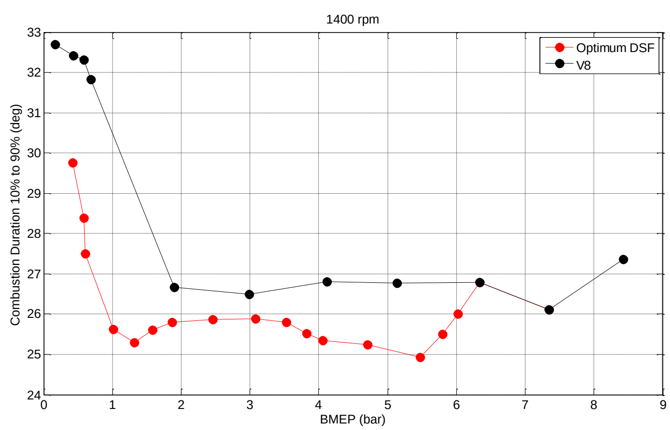

Figure 13: Combustion duration 10% to 90% (deg) of V8 and DSF operation at 1400 rpm

Pollutant Emissions

There are several experimental and theoretical works regarding engine emissions map [12-15]. The consensus of the literature is that at low loads BSCO, BSCO$_2$, and BSHC are higher than intermediate and high loads. Lower loads have higher BSFC (see Figure 6) causing higher specific emissions for CO, CO$_2$, and HC. The other reason is higher probability of unstable combustion and misfiring at low loads. Combustion instability can cause misfiring or incomplete combustion which is a major source of CO and HC emissions. BSCO$_2$ depends on engine load and stoichiometry of the mixture.

Brake specific production of CO, CO$_2$, HC, and NO$_x$ were measured during these experiments. For all experiments, equivalence ratio is held at approximately stoichiometric.

BSNO is strongly a function of combustion temperature, oxygen concentration, and engine load. Clearly, at higher loads due to higher temperature of the charge in the cylinder, NO emission will be higher. Also, the inhomogeneous mixing can cause leaner mixture in some zones which will boost NO production.

Figure 14 is the contour plots of BSCO map of engine at V8 and DSF operations. At low loads higher BSFC of V8 cause higher specific CO emissions. Figure 14 show that running engine with DSF mode reduces CO emission significantly. There can be two reasons for that. The first reason is higher thermal efficiency of engine which naturally results lower BSCO. The second one is complete combustion at low loads due to higher charge mass inside the cylinder. By running DSF at low loads (bmep < 1 bar), there is a reduction of CO emissions of approximately 60%.

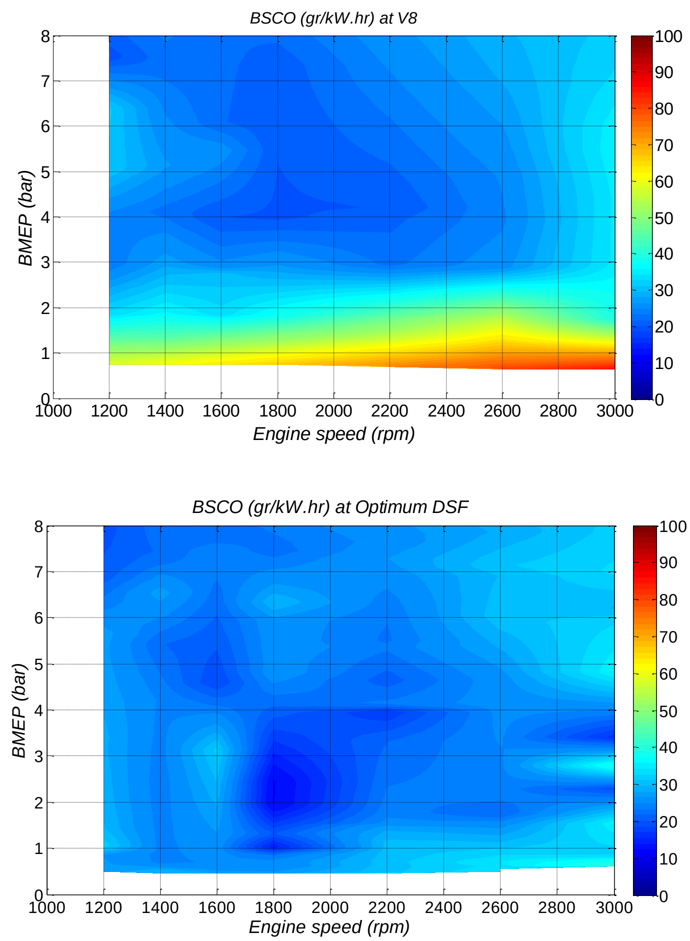

Figure 14: BSCO map of engine with V8 and DSF operations

The contour map of CO$_2$ emissions is presented in Figure 15. This figure also shows the specific CO$_2$ emissions. At low loads, higher thermal efficiency concludes lower BSCO$_2$. There is about 70% of BSCO$_2$ reduction at low loads. At higher loads due to almost identical thermal efficiencies, there is not a significant difference in BSCO$_2$.

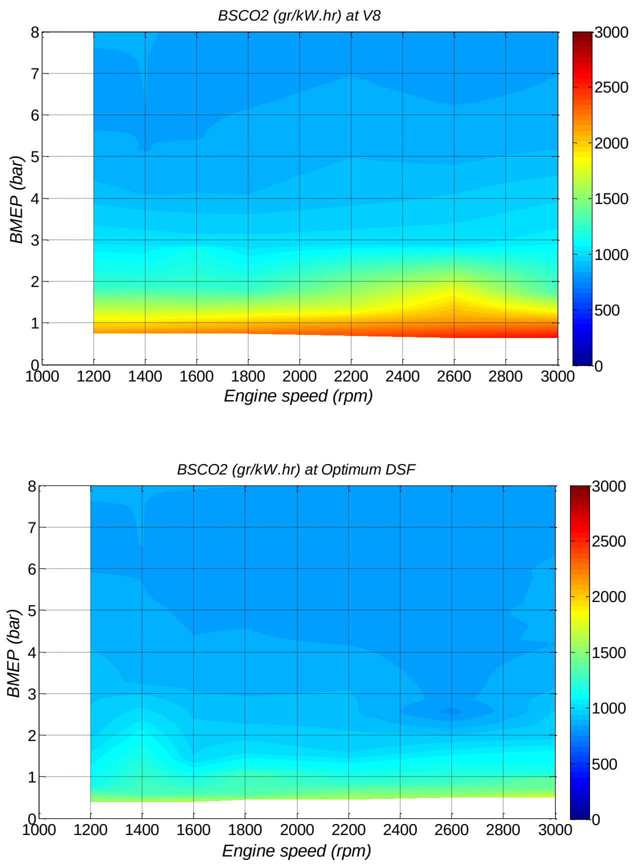

Figure 15: BSCO₂ map of engine with V8 and DSF operations

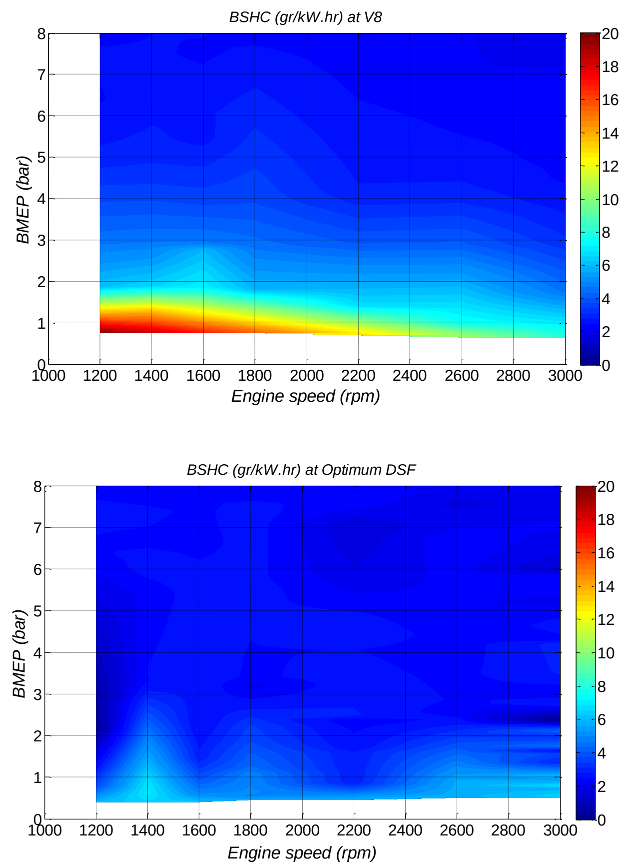

Figure 16: BSHC map of engine with V8 and DSF operations

Figure 16 shows the contour plots of BSHC as a function of bmep and engine speed. At low loads higher thermal efficiency of DSF decreases the concentration of unburned hydrocarbons. In addition, high probability of incomplete combustion at low loads for V8 can cause higher unburned hydrocarbons. Unburned hydrocarbons are also produced when the fuel/air mixture is pushed into crevices and then quenched at high pressures. It should be noted that DSF decreases the number of active cylinders; meaning that the number of quenching events in engine will decrease accordingly. This will cause lower unburned hydrocarbons than V8.

NOx emissions are one of major pollutants in spark ignition engines. Any attempt in increasing the thermal efficiency, reduction of oxygen concentration, and reduction of combustion temperature will reduce NOx. Clearly, DSF increases thermal efficiency especially at low loads. Figure 17 is showing the contour plots of BSNO as functions of bmep and rpm. It is shown that in some regions of low loads, V8 produces lower NOx than DSF. As it was mentioned earlier at bmeps <1 bar at V8, the cylinders can probably experience poor combustion. Consequently the combustion temperature will drop followed by lower NOx production. DSF usually takes place at intermediate rpms (1200-1600 rpm), at these conditions Figure 17 shows that BSNO at DSF is lower than V8. However, higher concentration of NOx at DSF can be reduced by proper after-treatment of exhaust gases.

Figure 18 shows the inlet gas temperatures into the left and right bank catalysts for DSF and V8 operation. Conversion efficiency of catalysts is strongly a function of temperature. At higher temperatures the conversion efficiency of catalyst increases significantly [10, 16]. Higher conversion efficiencies will reduce NOx, CO, and HC emissions. Figure 18 shows that DSF operation will increase the inlet gas temperature to the catalyst. It means that DSF operation will result a more efficient after-treatment of emissions. In Figure 18 we have plotted the minimum and maximum possible temperatures within 2% of best BSFCs. It shows that different firing densities will cause different temperatures. Nevertheless, the DSF temperatures are always higher than V8 operation.

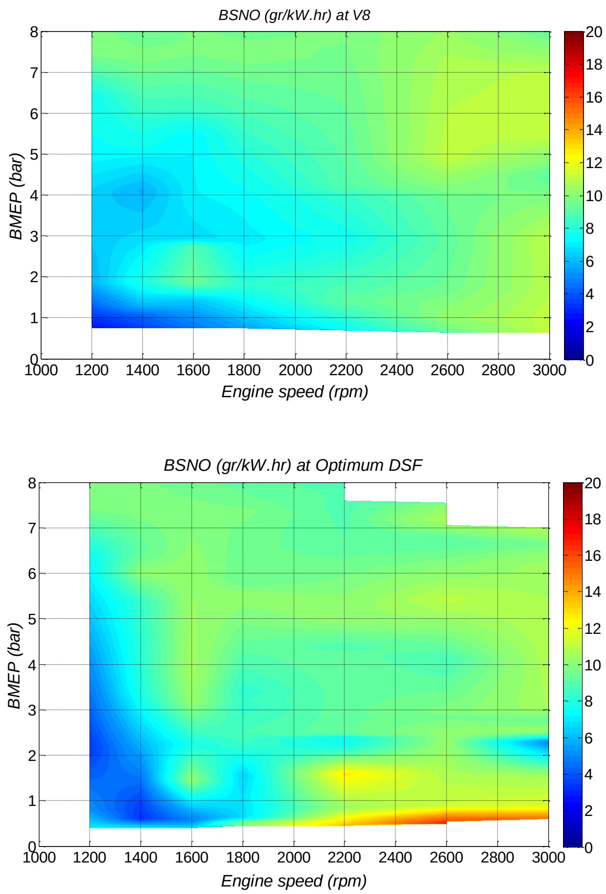

Figure 17: BSNO map of engine with V8 and DSF operations

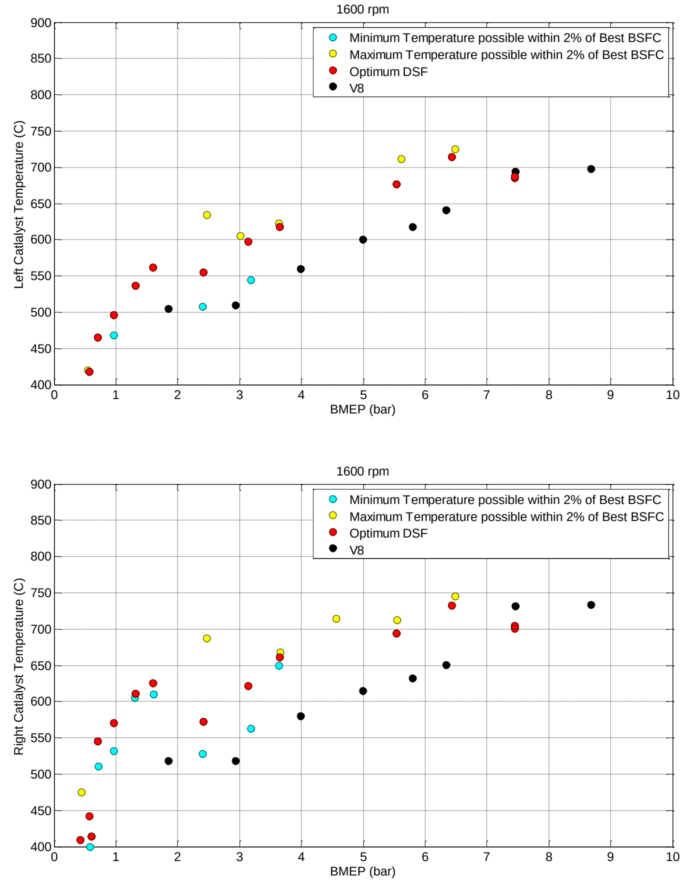

Figure 18: Inlet gas temperature into the left and right bank catalysts for DSF and V8 operations

Summary and Conclusions

1. Dynamic Skip Fire (DSF) reduces the pumping losses while it improves the combustion stability in spark ignition engines. Significant fuel economy gains, of approximately 18% over V8, have been achieved by operating an engine using Dynamic Skip Fire. DSF implementation does not require major modifications to the engine architecture; rather, it only requires valve deactivation.

2. DSF operation has a direct impact on combustion stability of the engine. Low loads at V8 require very low air mass in each cylinder. Low charge mass in the cylinders will cause combustion instability. With an intelligent calibration, DSF enhances combustion stability by increasing the mass of air in active cylinders. DSF improves the burning rate of the mixture which will boost the thermal efficiency.

3. DSF reduces CO, CO_2, HC, and at some conditions NOx emissions. The reduction is achieved through higher thermal efficiency and increased in-cylinder loading when in DSF

operation. In addition, DSF increases the temperature of the catalyst which will result higher conversion efficiency.

References

1. Stabinsky, M., Albertson, W., Tuttle, J., Kehr, D. et al., "Active Fuel Management™ Technology: Hardware Development on a 2007 GM 3.9L V-6 OHV SI Engine," SAE Technical Paper 2007-01-1292, 2007, doi:10.4271/2007-01-1292.
2. Hadler, J., Neusser, H.-J., Szengel, R., Middendorf, H., “The New TSI”, 33rd International Vienna Motor Symposium, April 2012.
3. Fujiwara, M., Kumagai, K., Segawa, M., Sato, R. et al., “Development of a 6-Cylinder Gasoline Engine with New Variable Cylinder Management Technology,” SAE Technical Paper 2008-01- 0610, 2008, doi:10.4271/2008-01-0610.
4. Förster, H.J., Lübbing, B.E., Letsche U., “Process and Apparatus for Intermittent Control of a Cyclically Operating Internal Combustion Engine”, U.S. Patent 4509488, 1982.
5. Serrano, J., Routledge, G., Lo, N., Shost, M. et al., "Methods of Evaluating and Mitigating NVH when Operating an Engine in Dynamic Skip Fire," *SAE Int. J. Engines* 7(3):1489-1501, 2014, doi:10.4271/2014-01-1675.
6. Wilcutts, M., Switkes, J., Shost, M., and Tripathi, A., "Design and Benefits of Dynamic Skip Fire Strategies for Cylinder Deactivated Engines," *SAE Int. J. Engines* 6(1):278-288, 2013, doi:10.4271/2013-01-0359.
7. Wyszynski, L., Stone, C., and Kalghatgi, G., "The Volumetric Efficiency of Direct and Port Injection Gasoline Engines with Different Fuels," SAE Technical Paper 2002-01-0839, 2002, doi:10.4271/2002-01-0839.
8. Ohata, A. and Ishida, Y., "Dynamic Inlet Pressure and Volumetric Efficiency of Four Cycle Four Cylinder Engine," SAE Technical Paper 820407, 1982, doi:10.4271/820407.
9. Chien, L., Younkins, M., and Wilcutts, M., "Modeling and Simulation of Airflow Dynamics in a Dynamic Skip Fire Engine," SAE Technical Paper 2015-01-1717, 2015, doi:10.4271/2015-01-1717.
10. Heywood, J.B., “*Internal Combustion Engine Fundamentals*.” McGraw-Hill, 1988.
11. Chen, S., Chien, L., Nagashima, M., Van Ess, J. et al., "Misfire Detection in a Dynamic Skip Fire Engine," *SAE Int. J. Engines* 8(2):389-398, 2015, doi:10.4271/2015-01-0210.
12. Ferrari, G., Onorati, A., D’Errico, G., Cerri, T. et al., "An Integrated Simulation Model for the Prediction of S.I. Engine Cylinder Emissions and Exhaust After-Treatment System Performance," SAE Technical Paper 2001-24-0045, 2001, doi:10.4271/2001-24-0045.
13. Wu, Y.Y., Chen, B.C., Tran, A.T., “Pollutant Emission Reduction and Engine Performance Improvement by Using a Semi-Direct Injection Spark Ignition Engine Fuelled by LPG”, *Aerosol and Air Quality Research*, 12: 1289–1297, 2012.
14. D'Errico, G., Ferrari, G., Onorati, A., and Cerri, T., "Modeling the Pollutant Emissions from a S.I. Engine," SAE Technical Paper 2002-01-0006, 2002, doi:10.4271/2002-01-0006.
15. Dordaei, H., Hazhir, A., and Eisazadeh-Far, K., "Pollutant Emissions Study of Gas Fueled SI Engines," SAE Technical Paper 2005-01-3790, 2005, doi:10.4271/2005-01-3790.
16. Kašpar, J., Fornasiero, P., Hickey, N., “Automotive catalytic converters: current status and some perspectives,” Catalysis Today 77 (2003) 419–449.

Contact Information

The contact information of the first author is:
eisazadehk@tulatech.com

Acknowledgments

The authors are grateful for all Tula Technology team. In particular this paper has been provided by helpful comments and contributions of Xin Yuan, Li-Chun Chien, Mark Wilcutts, and Chris Chandler.